Influence of delamination on fatigue properties of a fibreglass composite

Chiara Colombo *, Laura Vergani [1]

Politecnico di Milano, Department of Mechanical Engineering, Via La Masa 1, 20156 Milano, Italy

Article history:
Available online 18 July 2013

1. Introduction

Composite materials, especially reinforced in glass fibres, are widely used in structural applications, for their well-known favourable strength-to-weight ratio. Due to their heterogeneous nature and depending on the manufacturing process, composites present, however, a variety of defects or imperfections which can lead to different failure modes. Stiffness and strength of composites are directly related to the presence of such defects and the prediction of the residual fatigue life still remains an open issue.

Nevertheless, for structural composite parts of aeronautical, naval and transport industries, verification of fatigue strength and life prediction are fundamental for design and dimensioning.

The problem is complicated: the existence itself of a fatigue strength limit for composite materials is not clearly defined in the literature.

Some authors [1] do not find drastic change between low cycle fatigue and high cycle fatigue behaviour in composites, at the contrary of metals. In [2], high cycle fatigue tests are carried out on carbon and glass fibre reinforced composites, but identification of a fatigue limit is not clearly proposed, although other publications do not deny its existence. For instance, [3] studied unidirectional carbon fibre reinforced plastics and, considering the plot $\mathrm{Log}\,\varepsilon_{\max}$ – $\mathrm{Log}\,N_f$, an infinite life region was evidenced, where damage mechanisms are either arrested or have too low rates of progression to cause failure in a large number of cycles. Also in [4], where a pultruded glass fibre reinforced composites was studied, a fatigue limit of approximately 25% of the ultimate tensile strength was observed at ten million cycles.

Besides, damage tolerant design considerations for composite components are rarely followed due to this lack of knowledge. In the design stage, but also to properly plan non-destructive controls, material laws or experimental methodologies are, in fact, needed to provide estimation of residual lifetime and/or loading capacity. Knowledge of damage evolution in composite structures during fatigue loading is therefore crucial for a good design with composite materials. Identification of a parameter able to describe damage initiation and evolution would support designers in the choice of suitable materials and dimension for components.

The problems are really complex and it is not realistic to think dealing with all of them.

The aim of this paper is to consider some aspects related to the identification and monitoring of a parameter able to characterise the high cycle fatigue behaviour of a fibreglass composite. In particular, the effect of known specific defects present in the material has been considered.

A variety of damage evolutions and failure modes can occur in a composite structure: matrix cracking, fibre–matrix interfacial bond failure, fibre breakage, void growth, matrix crazing and delamination [5]. Among these failure mechanisms, in the present work attention is focussed on the last one: delamination, that is layers separation resulting in significant loss of mechanical properties. Delamination in composite structures can be induced, for instance,

* Corresponding author. Tel.: +39 02 2399 8667; fax: +39 02 2399 8263.
E-mail addresses: chiara.colombo@polimi.it (C. Colombo), laura.vergani@polimi.it (L. Vergani).
[1] Tel.: +39 02 2399 8249; fax: +39 02 2399 8263.

by the combination of external loadings with manufacture imperfections, accidental impacts [6], or even presence of active embedded sensors [7].

In the present paper a stress and thermal based approach is used to monitor delamination influence on fatigue life of a glass fibre reinforced plastic (GFRP). In the literature, many laws to estimate fatigue behaviour of fibreglass composites have been proposed, starting from experimental observations and obtaining analytical solutions: [8] considered a strain based approach and showed the existence of a fatigue limit for unidirectional, cross-plied and angle-plied laminates. In [9], a hierarchical and a synergistic strategy are proposed for multi-scale modelling of the damage evolution in the context of deformational response. Focusing on delamination aspect [10] presented an experimental work on the influence of delamination on stiffness, strength, and fatigue life, and fracture mechanics approach is adopted to describe global composite behaviour. Many other works have also been developed describing damage, and in particular delamination, evolution from the global standpoint of residual strength or stiffness; for instance, [11] analysed the behaviour of a carbon fibre reinforced composite with multiple delaminations in compression.

Dealing with delamination and composite toughness, experimental studies in the literature are mainly dedicated to mode I (crack opening) or II, including artificial layers acting as delamination onsets: experimental tests in this direction are also indicated in ASTM standards [12,13].

Recently, a work by [14] proposes an experimental stress-based study on the influence of delamination in carbon fibre reinforced composites, where delaminations are artificially induced in specimens. Fatigue tests are performed and variations with respect to undamaged specimens are evaluated in S–N curves and residual stiffness, for different stress ratios.

Based on this idea of introducing in the material a controlled and localised delamination, in the present study the mechanical static and fatigue behaviour of a GFR composite is investigated in delaminated condition. Comparisons are proposed with undamaged material, already presented and discussed in [15]. Innovative features of the work are not only the quantification of fatigue life-span reduction due to the presence of a delamination, but also the possible identification of a high cycle fatigue limit characteristic of the studied material.

From these considerations, in parallel with mechanical tests, in the present paper thermographic observations are also presented, with the aim of identifying temperature variation during the performed tests and to quantify a possible relation between temperature and fatigue life of the composite. Details of this experimental technique and its relation with fatigue behaviour, as present in the literature, are discussed in the following paragraph.

1.1. Thermographic approaches in literature

Among possible failure modes, delaminations are dangerous since they are not visible on the external surfaces of the composite structure. Adequate experimental techniques are therefore necessary to detect and monitor their location and evolution during loading. In the present paper infrared thermography is selected, since it is a non-contacting and non-destructive experimental methodology. Thermographic approaches are present in the literature to study behaviour of different composite materials, and to relate their thermal behaviour to fatigue life, from almost 40 years. In [16] an experimental study on a fibreglass reinforced material similar to the one studied in the present paper is taken into account. Indeed, thermal answer of the material under static or dynamic loads is directly related to its elastic or inelastic response. As proposed in [16], composite heating and elastic modulus decrease are correlated during fatigue life: early fatigue damage is widespread through the volume, and it is characterised by many small damage sites contributing both to global temperature raise and stiffness degradation. On the contrary, later fatigue damage is related to the coalescence of more defects in one, or enlargement of a main damage, resulting in a quick local increase in temperature as well as a loss in stiffness. With the development of interest in thermal analysis and related equipment, further considerations were proposed in the literature with the aim of quantifying by thermography fatigue life and variations in residual strength.

Three experimental methods to evaluate fatigue limit are proposed in the present paper, taken from experimental observations proposed in the literature: the first one is based on static loading of the specimens, other two are derived from the dynamic load application at variable stress levels.

Considering static loads, composites, as all other homogeneous materials, experience a decrease in surface temperature: this is the well-known thermoelastic effect [17] related to the variation in volume during elastic stage. After this initial decrease in temperature, while load increases, temperature deviates from linearity, till a minimum, then it starts to increase. From these experimental observations, some authors related the end of thermoelastic stage to fatigue limit of homogeneous materials [18], or to composite fatigue strength. This value of stress, which can be identified by thermal observations, was named σ_D, where D stands for damage initiation. This idea was developed for glass [15] and for basalt [19] fibre reinforced composites by authors of the present paper. In both these cases, if the applied load is lower than σ_D, defects present in the materials seem inactive and global temperature trend during tensile static tests is linear.

Together with this application of thermography, also dynamic loads can be taken into consideration, since during fatigue surface temperature of the specimens tends to reach an asymptotic value, characteristic of the stress level. Also, initial thermal answer to dynamic loads, that is the increase of temperature (ΔT) during cycling (ΔN), is a feature of the observed material and it can be related to the applied stress. According to the literature, values of $\Delta T/\Delta N$ plotted in function of different applied stresses present a double linear trend [20]. Intercept between these two lines, the breakup point, identifies a stress level, which is experimentally found to be near to the fatigue limit. This experimental observation was confirmed not only for homogeneous materials, but also for composites [19].

Moreover, a third method, based on progressively increased stress amplitudes and on energetic observations, was proposed by [21]. It is well known and proven that the dissipated energy is produced when the material starts being damaged, since it is related to irreversible loss of energy, such as inner friction of the material or irreversible damage evolution. In this case, locally shear stresses are self-generated in the material, but they cannot be identified by the classical thermal stress analysis (TSA), based on the consideration that temperature variations are proportional to the sum of the principal stresses, when adiabatic and reversible conditions are achieved during cyclic load application [22]. In this case, indeed, sum of principal stresses is null (principal stresses are equal and their signs are opposite). In that paper, a new digital processing technique, called D-mode, is proposed to evaluate the dissipated energy. It extracts non-linear coupled thermo-mechanical effects during cycling. Dissipated energy is much smaller than thermo-elastic source and therefore requires a high sensitive thermal imaging camera, such as a lock-in amplifier collecting both thermal and mechanical load signals. Its evaluation also requires a dedicated algorithm, which separates the dissipated energy from the thermo-elastic source and filters signals based on Fourier Transform analysis of thermal images.

According to experimental observations by this author [21], in case of progressively increased stress amplitudes, the dissipated

energy shows a bi-linear trend. When stress amplitude is low, dissipated energy in function of applied stress shows an almost flat trend, thus no energy is dissipated by irreversible mechanisms. Then, a rapid increase in the slope occurs for higher stress amplitudes. The author proposed that this breakup stress in the dissipated energy trend corresponds to a different behaviour in the material damage, thus it indicates damage initiation in the material during dynamic loads: he correlated it with the material fatigue limit. This consideration has recently been validated also for carbon fibre reinforced composites [23].

2. Tested material

Object of study is a glass fibre reinforced composite, made of non-crimp glass fibres (600 g/m^2) and epoxy resin (Epikote® Resin L1100, with 20% of 294 and 80% of 295 Epikure® Curing Agents). Laminates are manufactured by vacuum infusion process; stacking sequence is $[\pm 45]_{10}$. One initial plate without defects was manufactured and experimental tests were performed and described in [15]; fibre content was 50% in volume. Specimens coming from this plate are identified in the following with the letter S.

In the present paper, a second plate of the same composite material, characterised by the aforementioned symmetrical stacking sequence, is manufactured. In this laminate, fibre content is 55% in volume and nominal thickness is 4.4 mm. At a half of the plate thickness, a Teflon (PTFE) tape, 20 mm width and 0.1 mm thick, is placed during manufacturing to avoid complete resin adhesion between the 5th and the 6th layers. In this way, an artificial controlled delamination is created, which is similar for all the specimens. From the delaminated plate, rectangular specimens are obtained, identified with the letter T: Fig. 1 shows dimensions of the specimens, in accordance with ASTM D 3518; specimens are provided with tabs, to avoid stress concentration at the grips. In this figure, delamination location is shown, placed in the middle of the laminate thickness.

Fig. 2a shows a detail of the delaminated region in the specimen. As it is possible to see, Teflon layer is clearly visible by naked eyes on both sides of the laminate. Also, by carefully looking through the specimen thickness, the delaminated layer can be detected (Fig. 2b). Teflon insert appears white, and glass fibre laminates are partially transparent: by means of a simple backlighting, it is indeed possible to check the presence or absence of inner defects or delaminations in this material.

3. Experimental tests and equipment

In order to evaluate the difference in mechanical properties of non-delaminated and delaminated materials, different experimental tests are performed by means of a MTS Lankmark servo-hydraulic universal testing machine, equipped with a 100 kN load cell

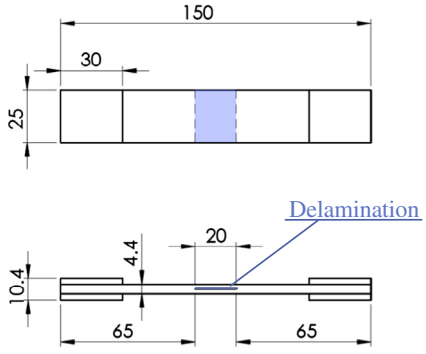

Fig. 1. Dimensions of specimens in mm.

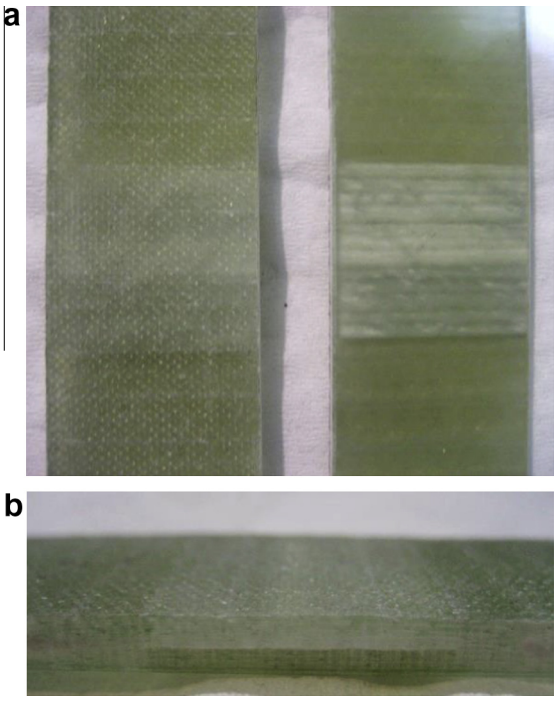

Fig. 2. (a) Front and rear view, and (b) through thickness view of a delaminated specimen before testing.

(Fig. 3). Three kinds of tests are performed: (1) static tests; (2) fatigue tests; and (3) stepwise tests.

Static and stepwise tests are thermally monitored by means of a IR-thermal camera (FLIR, model: Titanium SC7000), which is placed in front of the specimen at around 300 mm from the surface to be observed. The scanned region corresponds to the central part of the specimen, since regions at the extremities can be affected by heat transfer from grips.

Fig. 3. Experimental setup: testing machine and thermal equipment.

In this way, not only mechanical properties can be evaluated, but also thermal behaviour of the composite can be detected in the meantime, at least in the surface region. During experimental tests, the thermal camera is connected to a laptop and set to record not only matrices of surface temperatures, but also a reference signal from the load cell of the testing machine by a lock-in module, so that the two records from testing machine and thermal camera can be synchronised. In case of cyclic load applied to the specimen, so during stepwise tests, force signal from load cell is used by the lock-in module to measure more precisely the peak to peak temperature change, in terms of phase and amplitude, with respect to the modulated input cycle in terms of load.

In order to have a reference signal lower than 5 V, allowing the Lock-in module to filter the background noise, the camera was connected to load cell of the testing machine.

Finally, data post-processing is performed by Altair, a FLIR software: it allows to easily analyse thermal maps and to detect damaged zones. Also, in this software D-mode module is implemented.

Static tests are performed following ASTM D3518 standard in displacement control mode, setting cross-head speed at 2 mm/min; stress-time data from testing machine and temperature–time data from thermal camera are recorded at a frequency of 5 Hz.

Fatigue tests at constant stress amplitude are performed in accordance to ASTM D3479 standard, in load control. These tests are carried out taking into account different stress levels in order to get information and plot the σ_{max} – Log$N$ curve, characteristic of the material in the finite life region. Runout limit to stop fatigue tests is chosen at 10^7 cycles. Stress ratio is chosen equal to 0.1, and the frequency was set at 25 Hz.

Stepwise tests are cyclic fatigue tests at variable stress amplitude, i.e. progressively increasing the applied load. As for fatigue tests, stepwise tests are performed in load control, at constant stress ratio equal to 0.1 and a load frequency of 20 Hz; thermal data acquisition frequency is set at 25 Hz. During this kind of tests, specimens are subjected to loads with maximum stresses ranging from 16 to 48 MPa, each one for blocks of 2×10^3 cycles. Maximum number of applied loading blocks is 15, during which the load is stepwise increased by 2 MPa.

4. Results of mechanical tests

4.1. Static tensile tests

Two specimens (T1 and T2) with Teflon insert are statically tested and thermally monitored, with very similar results. Ultimate static strength (UTS) for delaminated specimens, as reported in Table 1a, does not fall in the statistical range of the undamaged specimens (142.23 ± 8.03 MPa [15]). UTS values for delaminated specimens are slightly higher than the upper confidence limit of virgin material: this is due to the fact that virgin and delaminated specimens come from two plates with different fibre contents. This first experimental results indicate however that the introduced type of damage, i.e. delamination, has a very small or even null influence on the static strength of this kind of composite.

Table 1
Mechanical characteristics from static tests. (a) Untested specimens. (b) Runout specimens.

	UTS (MPa)	E (MPa)	σ_D (MPa)
T1	156	10,560	30
T2	154	10,630	32
Undamaged (average) [15]	142	9550	30
Specimen ID			
T12	152	10,980	26
T13	154	10,570	29

4.2. Fatigue tests

A summary of fatigue tests is reported in Table 2 and in Fig. 4. In Fig. 4 fatigue data are plotted in the dimensionless diagram σ_{max}/UTS – LogN_f: indeed, this kind of plot is useful to underline the linear trend of both undamaged and delaminated specimens. Mechanical fatigue behaviour of these two categories of specimens is very different. Undamaged material progressively increases number of cycles to failure with the decrease of applied stress amplitude, till reaching the runout limit. On the contrary, delaminated specimens show a very low increase of N_f with respect to applied stress, but only till 50 MPa. At 40 MPa and lower stress levels, indeed, specimens are considered as runout. Change in resulting number of cycles to failure is very abrupt and identifies two net regions with different fatigue behaviours. For delaminated specimens, therefore, a fatigue limit can clearly be identified at approximately 40 MPa. It is possible to hypothesise this value to be also the high cycle fatigue limit for specimens without delamination. From plots in Fig. 4, indeed, the non-delaminated specimens tested at 40 MPa were runout or failed at a high number of cycles.

If available fatigue data are fitted by a linear regression with intercept equal to 1, a comparison between undamaged and damaged specimens can be quantified in terms of slope:

$$\begin{aligned} &\text{Undamaged material}: \sigma_{max}/\text{UTS} = -0.1199 \log N_f + 1 \quad R^2 = 0.86 \\ &\text{Damaged material}: \sigma_{max}/\text{UTS} = -0.1633 \log N_f + 1 \quad R^2 = 0.80 \end{aligned} \tag{1}$$

Therefore, considering this kind of fitting, slope in case of delaminated material is 36% greater than slope of undamaged material. These straight lines of Eq. (1) are included in plot of Fig. 4.

Both the two kinds of specimens, undamaged and delaminated, show a small scatter in fatigue data.

4.3. Static tensile tests on runout specimens

After fatigue tests, some of the runout specimens are also used for further static tensile and stepwise tests. Aim of this additional experimental tests is to evaluate the residual static strength and stiffness of the composite material and to estimate the induced damage after fatigue cycling. T12 and T13 specimens are selected for static tensile tests, while T10 and T11 for stepwise tests. Results of these specimens will be presented and discussed in the following paragraph.

Table 1b shows the results of static tests thermographically monitored. Residual strength from static tests on runout specimens is very similar to the un-cycled specimens, as well as elastic modulus: these two parameters are therefore not affected by the fatigue cycling at 30 and 20 MPa, below fatigue limit.

Table 2
Fatigue results.

Specimen ID	σ_{max} (MPa)	N_f (cycles)
T3	90	847
T4	90	1226
T5	70	2423
T6	70	2460
T7	50	6456
T8	50	7780
T9	50	10,197
T10	40	Runout
T11	30	Runout
T12	30	Runout
T13	20	Runout

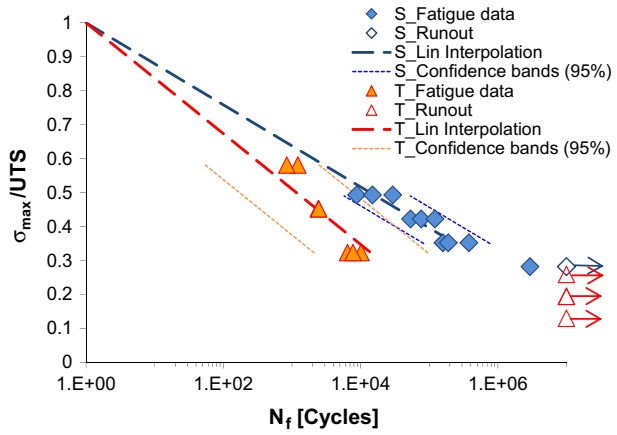

Fig. 4. Results of fatigue tests: σ_{max}/UTS – LogN_f plot.

5. Results of thermographic observations

5.1. Static approach

Considering thermal data collected during static tensile tests, it is possible to check the thermal answer of the specimen surface, and to relate it to a characteristic stress value σ_D, as described in Section 1.1.

If for S specimens the whole region was selected to plot stress and temperature vs. time curves [15], for delaminated specimens the regions to be analysed are carefully selected considering the upper and lower extremities of the Teflon layer, as shown in Fig. 5, respectively named area 1 and 2. A third region is also selected for comparison with the previous ones in the lower part of the specimen (area 3): this region can be considered as undamaged.

As shown in Fig. 5, during the test, surface temperature varies and different considerations can be proposed together with stress trend, plotted in Fig. 6a. In the first 20 s of testing, temperature decreases of 0.18 °C, but afterwards it increases till the end of test. Around approximately 100 s after the beginning of the test, some flashes of light (local heating in dot shape) are visible from thermal maps: they correspond to an irreversible damage, localised near the surface. These confined heating points, which are detectable both in S and T specimens, can be local failures occurring at the interface between fibre and matrix, i.e. debonding. Finally, during the last part of the test, specimen heats up to 10 °C, especially in the most damaged and delaminated regions, the central part.

Some differences in temperature trends for the three considered regions can be pointed out from plots in Fig. 6a and b. In these figures, temperature plots are obtained averaging on the selected area the surface temperatures. Moreover, plot is referred to temperature variation with respect to the initial value of temperature.

Considering Fig. 6a, and as shown in the last image of Fig. 5, area 3 is the hottest at the end of test, even if it is an undamaged region. Different regions for thermal maps are analysed, and slight differences in the areas selection can be detected. Considering initial instants of test as in Fig. 6b, indeed, area 1 presents a different trend with respect to the previous ones. In this graph, it is possible to easily detect that area 2 and 3 have an overlapped trend, while area 1 has a lower decrease in temperature. Approximately in the first 5 s of the test, these trends are very similar, but in the followings area 1 deviates. However, despite these analyses, it is never possible to clearly localise the presence of the delaminated Teflon layer.

In the instants where the three curves are close to be overlapped, trend of temperature in function of time is linear, as confirmed from the good coefficient of linear regression (R^2 near to unit) added to the plot in Fig. 6b. In order to define the end of the linear region, data are added to the linear regression till R^2 increases: the procedure to define t_D and corresponding damage stress σ_D is therefore univocal. Obtained σ_D values are reported in Table 1a: they are near to σ_D found for S specimens and obtained by the same approach (30 MPa [15]). If for homogeneous materials σ_D is indicated in the literature as the fatigue limit, in the tested composite this thermographic method seems to underestimate the value obtained from fatigue curves of delaminated specimens (40 MPa).

As for untested T specimens, also for runout specimens T10 and T11, during static tensile tests surface thermal maps are collected, and, with the same approach, an estimation of the σ_D stress corresponding to the end of the thermoelastic phase is proposed. Table 1b shows these σ_D values: results. Comparing σ_D between untested and runout specimens, a slight decrease of approximately 10% can be evidenced. This reduction can be an indication of the decrease in residual fatigue life.

5.2. Stepwise approaches

From stepwise tests, mainly performed for thermal observations, two method of data analysis are followed, as discussed in the introduction. Fig. 7 shows an example: stress and temperature data are plotted in function of number of cycles; block progression is also indicated. After collecting data by the IR-thermal camera, temperature arrays are analysed by plotting ΔT in function of ΔN: curves are almost all linear in each considered block of cycles.

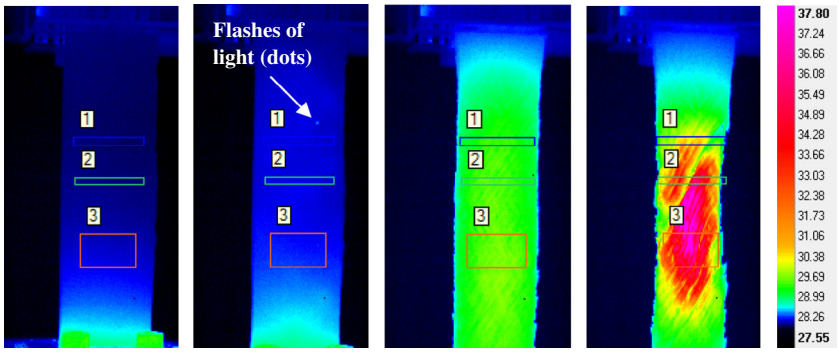

t = 0 s (beginning of test) | t = 105 s | t = 426 s (in correspondence of UTS) | t = 551 s (end of test)

Fig. 5. Thermal maps of a static test (specimen T2).

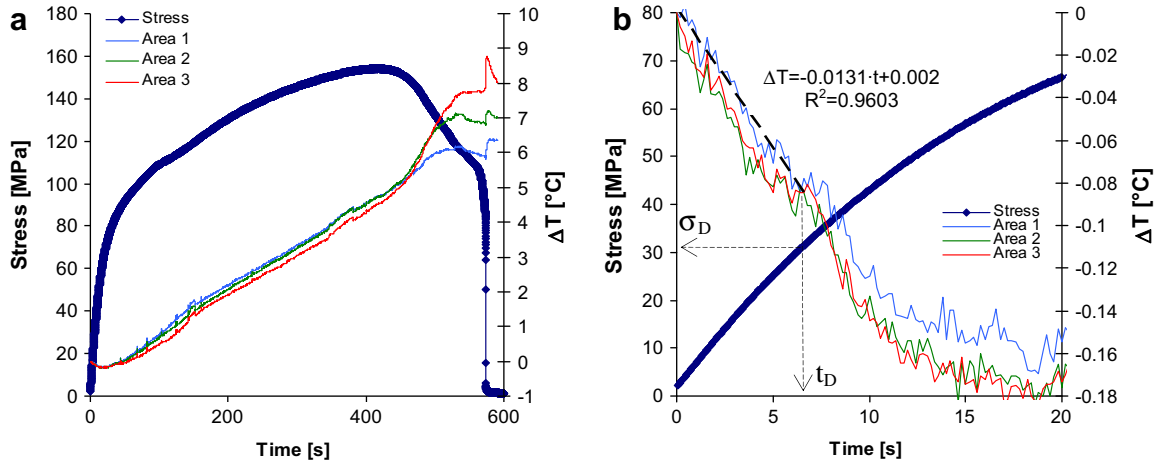

Fig. 6. Stress and temperature vs. time curves during a static test (specimen T2): (a) whole and (b) initial instants of static test.

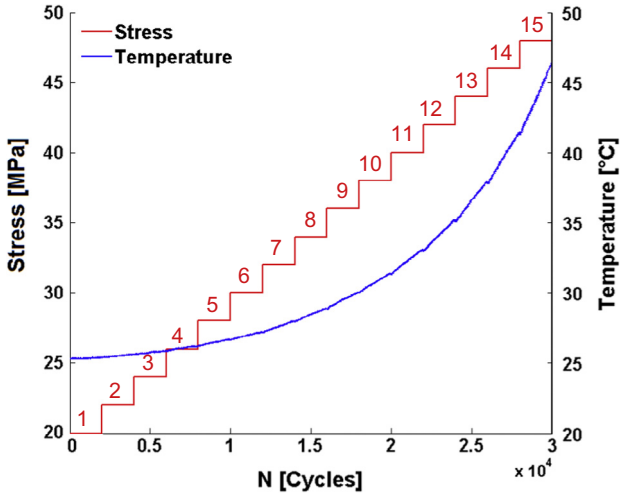

Fig. 7. Stepwise test on T14 specimen: stress and temperature trends.

Selected areas for analysis correspond, for all the specimens, to the whole region: similar trends are observed if other smaller regions are selected.

A linear regression is proposed for data fitting, and $\Delta T/\Delta N$ values are evaluated for each block at constant stress amplitude. These values are plotted in function of applied stress (σ_{max}) and shown in Fig. 8a, for all considered specimens. T14 and T15 are untested specimens with Teflon insert; T11 and T12 are two runout Teflon specimens; S1 is a characteristic trend of an undamaged specimen from [15], and S2 is an undamaged runout specimen at 40 MPa. It is clearly visible that, apart from the undamaged specimen S2, the trend observed for all the other specimens seems very similar. This can indicate that the damage level is similar if Teflon is present or if fatigue loadings are already carried out by the specimens. Plot in Fig. 8a is then divided into two linear curves and intercept identifies σ_D, as described in Section 1.1. Table 3 shows a summary of the evaluated σ_D stresses.

The same thermal matrices are also analysed by the dissipation mode (D-mode), which allows the evaluation of the dissipated energy by the monitored sample during fatigue cycling. Fig. 8b shows the evaluated dissipated energy in function of the applied stress σ_{max}. In this graph, the bilinear trend is more visible, since at the beginning the trend is very flat and the dissipated energy is near to zero. Increasing stress amplitude, on the contrary, induces a progressive raise in the dissipated energy. Also in this case, the trend is interpolated by two straight lines, and the intercept identifies σ_D stress shown in Table 3.

From the obtained values of Table 3, some considerations can be drawn: first of all, for each specimen, the two experimental methods based on thermal observations indicate very similar values for σ_D stress and the maximum difference is 8%.

Moreover, comparing estimations of σ_D from static and stepwise tests thermographically monitored, for each category of specimens, static method underestimates fatigue limit, while stepwise method gives a more realistic value, if compared to the fatigue results of delaminated specimens. Indeed, both for untested S and T specimens, high cycle fatigue limit is estimated around 38 MPa. This is an average stress between all the tested specimens. No difference in terms of σ_D can indeed be evinced between specimens with and without Teflon insert.

Since fatigue tests on T specimens evidenced the presence of a high cycle fatigue limit, and thermographic methods identify it, we propose that it can exist not only for T but also for S specimens. Moreover, thermography can be indicated as an useful tool to quickly estimate high cycle fatigue limit, avoiding an extensive testing programme.

Finally, some further considerations on runout specimens can also be drawn. The only runout S2 specimen tested at 40 MPa shows similar value of σ_D with respect to the S1 untested one. On the contrary, estimated σ_D of the two runout T specimens is lower than untested specimens with Teflon insert (−7% and −14% respectively for T11 and T10 specimens). This experimental data can indicate that the reduction in fatigue life after the application of a constant amplitude fatigue load is more marked on T specimens than S specimens.

6. Failure observations and discussion

Further observations, useful for interpreting experimental data, can be added for a discussion from an analysis of the S and T specimens by means of observations at the optical microscope. First of all, through-thickness images are collected on virgin material, before testing. As reported in Fig. 9a on undamaged virgin material, the 10 layers composing the laminate can clearly be detected, and a resin layer between plies is also visible. In Fig. 9b, instead, an image of the artificially delaminated composite is shown: also in this figure, layers are detectable, as well as the Teflon layer placed between 5th and 6th plies. From a magnification at the end of the Teflon layer, crack tip can be detected, which does not appear as a discontinuity in the material (Fig. 9c).

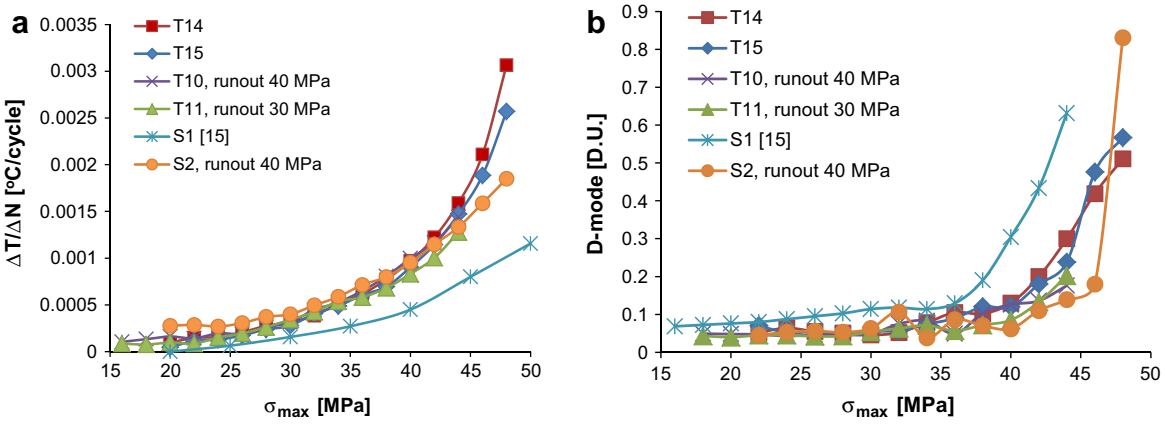

Fig. 8. Results of stepwise tests: (a) $\Delta T/\Delta N - \sigma_{max}$ and (b) D-mode-σ_{max} plots.

Table 3
Evaluation of σ_D from thermal stepwise observations.

Specimen ID	Type	σ_D (MPa) from $\Delta T/\Delta N - \sigma_{max}$	σ_D (MPa) from D-mode
T14	Delaminated, untested	39.5	39.0
T15	Delaminated, untested	40.1	40.6
T11	Delaminated, runout 30 MPa	34.5	37.4
T10	Delaminated, runout 40 MPa	33.6	33.7
S1 [15]	Non-delaminated, untested	36.7	37.2
S2	Non-delaminated, runout 40 MPa	36.1	39.9

Very similar images to those shown in Fig. 9 for untested material are collected also for the runout specimens, after 10^7 cycles. Fig. 10a shows a S runout specimen and Fig. 10b an artificially delaminated one. It appears interesting that delamination is fully closed and inactive (Fig. 10c), as at the beginning of the fatigue test (Fig. 9c). In this sense, it is possible to affirm that delamination is not activated for load amplitudes that bring specimens to runout: presence of Teflon layer is completely irrelevant for fatigue mechanical behaviour during these tests.

On the contrary, if attention is paid to failure regions of broken specimens during fatigue tests, two categories can be pointed out. If a specimen without insert is taken into account, in the central region of the broken specimen, all layers delaminate at approximately the same distance from grips, as shown in Fig. 11a. On the contrary, if Teflon layer is present, most of the broken specimens at 90, 70 and 50 MPa show a failure as in Fig. 11b: the five upper layers tends to maintain continuity in the material with respect to the lower symmetric part, and Teflon layer is pulled in opening conditions. One of the two crack tips (the one at left side of Fig. 11b) finally fails and all the layers explode and split, while the other side of the Teflon insert, on the right, reveals an active crack in propagation trough 5th and 6th layers (Fig. 11c). In general, therefore, for these specimens, presence of a pre-existing delamination in the composite deeply changes failure mode during fatigue testing. Indeed, it activates a preferential way for layers

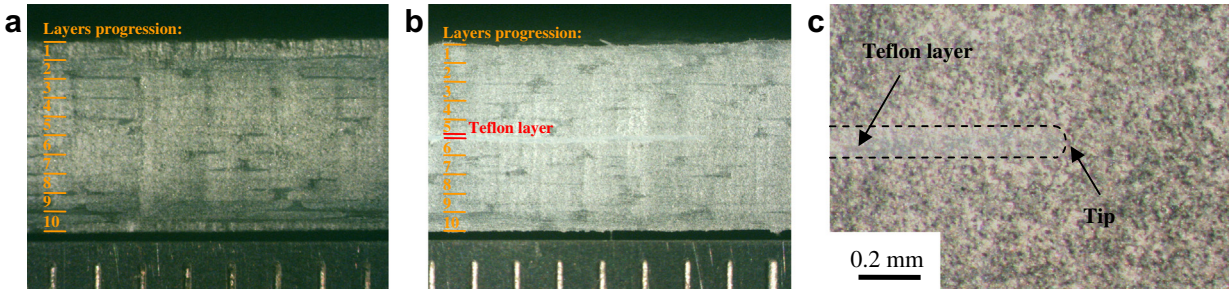

Fig. 9. (a) Undamaged and (b) artificially delaminated material before testing; (c) magnification in the tip region.

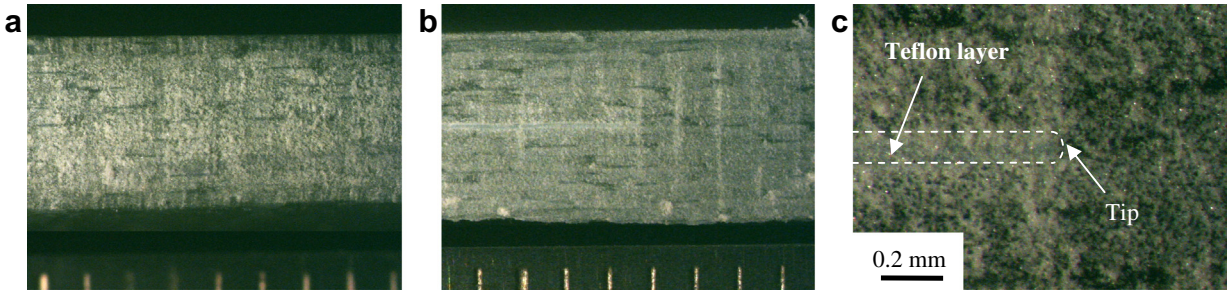

Fig. 10. Magnification of runout (a) S2 and T10 (b) specimens, σ_{max} = 40 MPa.

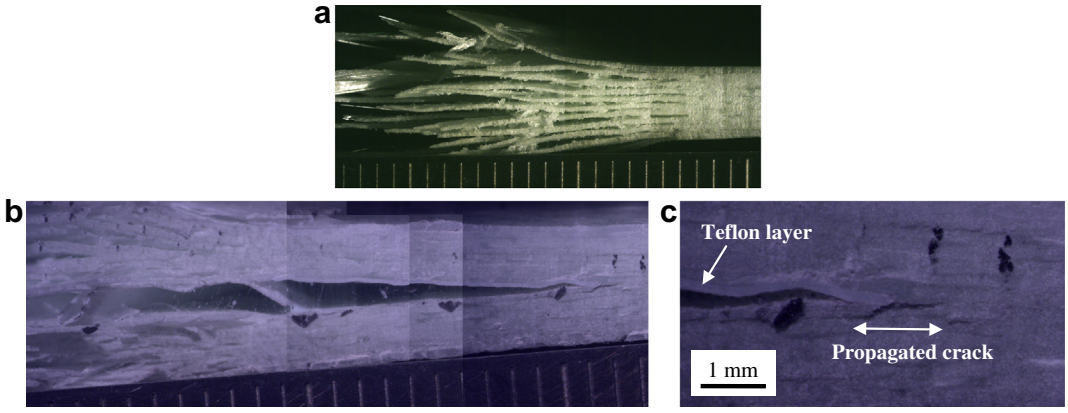

Fig. 11. Failure of (a) a S specimen and (b) T5 specimen after fatigue test; and (c) magnification in the tip region.

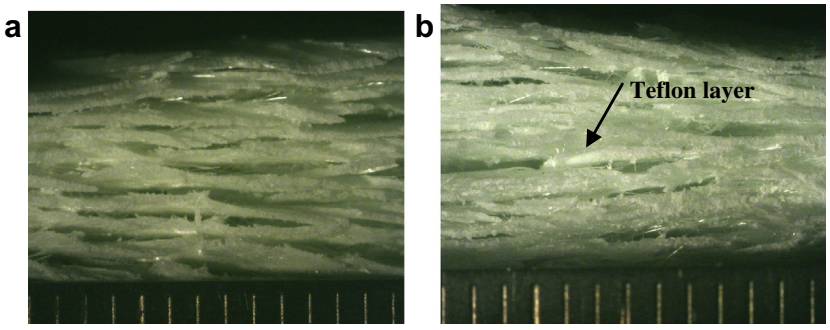

Fig. 12. Failure of (a) a S specimen and (b) T2 specimen after static test.

separation and definitively decreases the whole energy required to delaminate all layers of composite.

Failure mode of undamaged specimens during fatigue tests is very similar to the static one, both of damaged and undamaged specimens (Fig. 12). Indeed, as shown from results of experimental tests, static properties are comparable for both the two series of tested specimens: failure occurs delaminating all the 10 layers composing the composite laminate.

Images proposed in this paragraph have shown a possible explication of the failure mechanisms, occurring during static and fatigue tests on a classical laminate and on a initially delaminated composite. Energy required to delaminate composite plies can be divided in three levels:

(1) for runout specimens, energy available from loading cycling is not sufficient to delaminate layers, neither the Teflon one if present;
(2) for S specimens, delamination of all layers occurs simultaneously increasing the applied load, thus available energy;
(3) at an intermediate energy level, only delamination of Teflon layer, if present, is activated and it causes final failure of the specimen.

These images, therefore, add a physical interpretation to results of fatigue tests previously shown in Fig. 4. Shift in $\sigma_{max}/UTS - Log N_f$ curves between T and S specimens, shown in Fig. 4, can definitively be attributed to activation of Teflon delamination, starting from σ_{max} equal to 50 MPa. It seems, therefore, that above σ_D stress level, delamination is the main damage mechanism occurring during fatigue of T specimens. At 30 MPa and lower stress amplitudes, all tested specimens record runout. Between 30 and 40 MPa, a change in failure mechanisms occurs, and this is clearly visible for T specimens.

Seen in this light, also results from thermographic analyses can be useful to comment fatigue data. Indeed, σ_D can be a stress value identifying variation in damage mechanisms. According to the literature, composites undergo a progressive and continuous damage during fatigue cycling. This progressive micro-damage occurs below 30 MPa, high cycle fatigue limit or σ_D. If stress values higher than σ_D are considered in fatigue cycling, delamination phenomenon affects one or more layers and $\sigma_{max}/UTS - Log N_f$ curve changes slope.

7. Conclusions

In this paper experimental tests on a glass fibre reinforced composite were performed in order to better understand fatigue damage of this material, focusing attention on delamination and its influence on residual fatigue life. Delamination was induced in specimens by a Teflon insert in the mid-thickness. Surface temperature was also monitored during some experimental tests. From the proposed results and discussion, some considerations can be summarised in conclusion:

- from the mechanical point of view, tensile static properties are not affected by the presence of a delamination in the specimen. On the contrary, tests revealed that fatigue life is reduced by almost 40%. Moreover, delaminated specimens clearly showed the existence of a fatigue limit;
- from thermal observations during static and stepwise tests, three approaches revealed a relation between thermal response of the material and the fatigue limit. Thermography is therefore proposed as a tool to monitor damage initiation and its evolution during testing, and to quickly estimate fatigue life of composites;

- considerations on runout specimens based on the same thermal methods revealed that residual fatigue limit of delaminated specimens is reduced of more than 10%;
- images at the optical microscopy revealed that delaminations were inactive for runout specimens and no cracks were created in the specimens. When failure occurred, however, one of the sides of the delamination onset propagated and damage spread to all the other layers, thus the whole energy required to delaminate the composite was globally decreased.

Acknowledgements

Authors would like to thanks Prof. Gerhard Ziegmann and Dr. Sonja Niemaier from Technical University of Clausthal, and former student Alessandro Panizio from Politecnico for manufacturing the tested material.

References

[1] Bathias C. An engineering point of view about fatigue of polymer matrix composite materials. International Journal of Fatigue 2006;28(10):1094–9.
[2] Demers CE. Fatigue strength degradation of E-glass FRP composites and carbon FRP composites. Construction and Building Materials 1998;12(5):311–8.
[3] Gamstedt EK, Talreja R. Fatigue damage mechanisms in unidirectional carbon–fibre-reinforced plastics. Journal of Material Science 1999;34(11):2535–46.
[4] Keller T, Tirelli T, Zhou A. Tensile fatigue performance of pultruded glass fiber reinforced polymer profiles. Composite Structures 2005;68(2):235–45.
[5] Sawyer LC, Grubb DT, Meyers GF. Polymer Microscopy. third ed. New York, NY, USA: Springer; 2008.
[6] Kempf M, Schwägele S, Ferencz A, Altstädt V., 2011. Effect of impact damage on the compression fatigue performance of glass and carbon fibre reinforced composites. In: Proceedings of the 18th International Conference on Composite Materials (ICCM/18), Jeju Island, Korea, 21–26 August 2011.
[7] Butler S, Gurvich M, Ghoshal A, Welsh G, Attridge P, Winston H, et al. Effect of embedded sensors on interlaminar damage in composite structures. Journal of Intelligent Material Systems and Structures 2011;22(16):1857–68.
[8] Talreja, R., 1991. Fatigue of composite materials: damage mechanisms and fatigue-life diagrams. In: Proceedings of the Royal Society of London. Series A, Mathematical and Physical Sciences, vol. 378(1775), pp. 461–475.
[9] Talreja R. Multi-scale modeling in damage mechanics of composite materials. Journal of Materials and Science 2006;41(20):6800–12.
[10] O'Brien TK. Generic aspects of delamination in fatigue of composite materials. Journal of the American Helicopter Society 1987;32(1):13–8.
[11] Kutlu Z, Chang FK. Modeling compression failure containing multiple through-the-width delaminations. Journal of Composite Materials 1992;26(3):350–87.
[12] ASTM D5528-94a: Standard test method for mode I interlaminar fracture toughness of unidirectional fiber-reinforced polymer matrix composites.
[13] ASTM D6671/D6671M-06: Standard test method for mixed mode I-mode II interlaminar fracture toughness of unidirectional fiber reinforced polymer matrix composites.
[14] Reis PNB, Ferreira JAM, Antunes FV, Richardson MOW. Effect of interlayer delamination on mechanical behaviour of carbon/epoxy laminates. Journal of Composite Materials 2009;43(22):2609–22.
[15] Colombo C, Libonati F, Vergani L. Fatigue damage in GFRP. International Journal of Structural Integrity 2012;3(4):424–40.
[16] Nevadunsky JJ, Lucas JJ. Early fatigue damage detection in composite materials. Journal of Composite Materials 1975;9(4):394–407.
[17] Thomson W. (Lord Kelvin). On the thermoelastic, thermomagnetic and pyro-electric properties of matters. Philosophical Magazine 1878;5:4–27.
[18] Clienti C, Fargione G, La Rosa G, Risitano A, Risitano G. A first approach to the analysis of fatigue parameters by thermal variations in static tests on plastics. Engineering Fracture Mechanics 2010;77(11):2158–67.
[19] Colombo C, Vergani L, Burman M. Static and fatigue characterisation of new basalt fibre reinforced composites. Composite Structures 2012;94(3):1165–74.
[20] La Rosa G, Risitano A. Thermographic methodology for rapid determination of the fatigue limit of materials and mechanical components. International Journal of Fatigue 2000;22(1):65–73.
[21] Brémond P. IR imaging assesses damage in mechanical parts: determining the fatigue limit of real structures under real operating conditions saves time, Photonics Spectra 2004, www.photonics.com/Article.aspx?AID¼18123 (accessed 30.04.13).
[22] Greene RJ, Patterson EA, Rowlands RE. Thermoelastic Stress Analysis, Part C26. In: Sharpe WN, editor. New York: Springer Handbook of Experimental Solid Mechanics; 2008. p. 743–67.
[23] Montesano J, Fawaz Z, Bougherrara H. Use of infrared thermography to investigate the fatigue behaviour of a carbon fiber reinforced polymer composite. Composite Structures 2013;97:76–83.